

# Monitoring of the Forced Hydrolysis of FeCl<sub>3</sub> Solutions in the Presence of Sodium Dodecyl Sulphate

Mira Ristić,<sup>1,\*</sup> Jasenka Štajdohar,<sup>1</sup> Ivana Mitar,<sup>2</sup> Svetozar Musić<sup>1,3</sup>

<sup>1</sup> Ruđer Bošković Institute, Bijenička cesta 54, P.O. Box 180, HR-10002 Zagreb, Croatia

<sup>2</sup> Faculty of Science, University of Split, Ul. Ruđera Boškovića 33, HR-21000 Split, Croatia

<sup>3</sup> Croatian Academy of Sciences and Arts, Trg Nikole Šubića Zrinskog 11, HR-10000 Zagreb, Croatia

\* Corresponding author's e-mail address: ristic@irb.hr

RECEIVED: August 31, 2018 \* REVISED: October 15, 2018 \* ACCEPTED: November 26, 2018

**Abstract:** Precipitations by the forced hydrolysis of 0.2 M FeCl<sub>3</sub> aqueous solutions between 2 and 72 hours in the presence of 1 % sodium *n*-dodecyl sulphate (SDS) were investigated. In the absence of SDS a direct phase transformation  $\beta\text{-FeOOH} \rightarrow \alpha\text{-Fe}_2\text{O}_3$  via dissolution/recrystallization occurred in the precipitation system. In the presence of SDS small amounts (traces) of  $\alpha\text{-FeOOH}$  as an intermediate phase precipitated, and with a prolonged time of forced hydrolysis  $\alpha\text{-FeOOH}$  also transformed to  $\alpha\text{-Fe}_2\text{O}_3$  via the dissolution/recrystallization mechanism. On the basis of Mössbauer spectra it was concluded that in the presence of SDS the  $\alpha\text{-Fe}_2\text{O}_3$  phase exhibited a lower degree of crystallinity. During the precipitation process in the presence of SDS the competition between the stability of Fe(III)-dodecyl sulphate on one side and the formation of iron oxide phases on the other also played an important role. Thermal field emission scanning electron microscopy (FE SEM) revealed that the big  $\alpha\text{-Fe}_2\text{O}_3$  particles possessed a substructure. The elongation of primary  $\alpha\text{-Fe}_2\text{O}_3$  particles produced in the presence of SDS was noticed. This effect can be assigned to the preferential adsorption of sulphate groups on nuclei and crystallites of FeOOH and  $\alpha\text{-Fe}_2\text{O}_3$  phases during the forced hydrolysis of FeCl<sub>3</sub> solutions.

**Keywords:** FeCl<sub>3</sub> hydrolysis, sodium *n*-dodecyl sulphate,  $\alpha\text{-Fe}_2\text{O}_3$ ,  $\alpha\text{-FeOOH}$ , XRD, Mössbauer, FT-IR, FE SEM.

## INTRODUCTION

**H**EMATITE ( $\alpha\text{-Fe}_2\text{O}_3$ ) particles have found different applications as pigments, photocatalysts, electrode materials, fine abrasives and cosmetic additives.  $\alpha\text{-Fe}_2\text{O}_3$  can also be used as an adsorbent for toxic elements or radioisotopes in wastewater treatment. In surface and colloid chemistry these particles are often used as model systems due to their excellent acido-basic surface properties. The investigation of colloid stability of  $\alpha\text{-Fe}_2\text{O}_3$  particles is important to understand the nature of this phenomenon.

The simplest way to produce  $\alpha\text{-Fe}_2\text{O}_3$  particles is by forced hydrolysis in a boiling 0.01 M FeCl<sub>3</sub> solution,<sup>[1]</sup> whereas at temperatures below 70 °C akaganéite ( $\beta\text{-FeOOH}$ ) particles (spindle- or cigar-shaped) will precipitate. The synthesis and characterization of  $\beta\text{-FeOOH}$  and its

decomposition products in vacuum were investigated.<sup>[2]</sup> Musić *et al.*<sup>[3]</sup> used Mössbauer spectroscopy to investigate the hydrolysis of 0.1 M solutions of Fe(NO<sub>3</sub>)<sub>3</sub>, FeCl<sub>3</sub>, Fe<sub>2</sub>(SO<sub>4</sub>)<sub>3</sub> or NH<sub>4</sub>Fe(SO<sub>4</sub>)<sub>2</sub> at 90 °C. A proposal was made concerning the mechanism of formation of the hydroxides and oxides of Fe<sup>3+</sup> ions in these precipitation systems. It is generally accepted that the phase transformation  $\beta\text{-FeOOH} \rightarrow \alpha\text{-Fe}_2\text{O}_3$  in hydrolysing FeCl<sub>3</sub> solutions at elevated temperature is driven by a dissolution/ recrystallization mechanism.<sup>[4–6]</sup> The application of Mössbauer spectroscopy to investigate the precipitation of iron oxides has recently been reviewed by Musić *et al.*<sup>[7]</sup>

The nano / microstructure of  $\alpha\text{-Fe}_2\text{O}_3$  plays a very important role in many of its applications. For this reason many researchers investigated conditions for the preparation of  $\alpha\text{-Fe}_2\text{O}_3$  with different properties. Katsuki and Komarneni<sup>[8]</sup> used the forced hydrolysis of the FeCl<sub>3</sub> solution

at hydrothermal conditions to investigate the influence of morphology on the colour of the red pigment ( $\alpha$ -Fe<sub>2</sub>O<sub>3</sub>) in the production of porcelain. Sugimoto *et al.*<sup>[9]</sup> noticed remarkably different effects of Cl<sup>-</sup>, OH<sup>-</sup>, SO<sub>4</sub><sup>2-</sup> or PO<sub>4</sub><sup>3-</sup> anions on the shape and internal structure of  $\alpha$ -Fe<sub>2</sub>O<sub>3</sub> particles. Hollow  $\alpha$ -Fe<sub>2</sub>O<sub>3</sub> spheres were produced by the forced hydrolysis of the FeCl<sub>3</sub> solution containing H<sub>3</sub>PW<sub>12</sub>O<sub>40</sub>.<sup>[10]</sup> Mesoporous  $\alpha$ -Fe<sub>2</sub>O<sub>3</sub> particles were produced by the forced hydrolysis of the FeCl<sub>3</sub> solution containing L-phenylalanine and *N*-(3-di methylaminoethylaminopropyl)-*N*-ethylcarbodiimide hydrochloride.<sup>[11]</sup> Kandori *et al.*<sup>[12]</sup> also investigated the effect of surfactants on the precipitation of colloidal particles by the forced hydrolysis of the FeCl<sub>3</sub>-HCl solution. The hydrothermal transformation  $\beta$ -FeOOH  $\rightarrow$   $\alpha$ -Fe<sub>2</sub>O<sub>3</sub> in dense aqueous suspensions, prepared by a partial neutralization of the concentrated FeCl<sub>3</sub> solution with the concentrated NaOH solution, was investigated by Žic *et al.*<sup>[13]</sup> Žic *et al.*<sup>[14]</sup> also investigated the precipitation of  $\alpha$ -Fe<sub>2</sub>O<sub>3</sub> from dense  $\beta$ -FeOOH suspensions containing ammonium amidosulphonate. The peanut-type  $\alpha$ -Fe<sub>2</sub>O<sub>3</sub> particles, as well as particles in the form of double cupolas interconnected with the neck were obtained. These particles showed a substructure. Double cupolas were porous and consisted of linear chains of small  $\alpha$ -Fe<sub>2</sub>O<sub>3</sub> particles (also interconnected) which were directed from the centre towards the surface of cupolas.

The aim of the present work was to obtain more data about the influence of sodium dodecyl sulphate on the crystallization kinetics, phase transformations and particle morphology in the precipitates produced by the forced hydrolysis of aqueous FeCl<sub>3</sub> solutions. This work is a continuation of our longtime investigations in the precipitation chemistry of iron oxides (group name for hydroxides, oxyhydroxides and oxides of iron). In many cases the phase analyses of solid hydrolytical products of iron ions are a demanding task, specifically if iron oxide phases vary from amorphous to a well-crystalline nature. For this reason three complementary techniques, XRD, <sup>57</sup>Fe Mössbauer and FT-IR were used in the phase analysis. Generally, it is known that surface active agents act very differently on the precipitation processes in dependence on their characteristics (polar, nonpolar, chemical nature of the organic chain, pH).

## EXPERIMENTAL

### Sample Preparation

AnalaR grade FeCl<sub>3</sub>·6H<sub>2</sub>O was supplied by *Kemika*. Sodium n-dodecyl sulphate (SDS) was supplied by *Sigma Aldrich* (Cat. No.: 151-21-3; ACS grade reagent). Twice distilled water was prepared in own laboratory and used in all experiments. A stock solution 2M FeCl<sub>3</sub> was prepared. The

concentration of 0.2M FeCl<sub>3</sub> solutions was adjusted in all precipitation systems. Experimental conditions for the preparation of samples are given in Table 1. The yellowish precipitate was formed by adding the FeCl<sub>3</sub> solution to a clear aqueous solution of SDS, thus indicating the formation of Fe(III)-dodecyl sulphate. Thus obtained suspension was homogenized in an ultrasound bath. The precipitation systems were autoclaved at 160 °C using a Teflon<sup>®</sup>-lined, non-stirred pressure vessel manufactured by *Parr Instruments* (model 4744). The autoclaves were heated between 2 and 72 h in a DX 300 gravity oven (*Yamato*; temperature uniformity  $\pm 1.9$  °C at 100 °C and  $\pm 3$  °C at 200 °C). The autoclaving times were corrected for the time needed that the autoclave reaches the predetermined temperature. After a proper autoclaving time the autoclaves were abruptly cooled with cold water. The mother liquor was separated from the precipitate with the ultra-speed centrifuge (*Sorvall* model Super T21). The separated precipitates were subsequently washed with twice-distilled water and one time with C<sub>2</sub>H<sub>5</sub>OH, then dried.

### Instrumentation

XRD patterns were recorded with an APD 2000 powder diffractometer manufactured by *ItalStructures* (GNR Analytical Instruments Group, Italy).

<sup>57</sup>Fe Mössbauer spectra were recorded at 20°C in the transmission mode, using a standard configuration by *WissEl* GmbH (Starnberg, Germany). The <sup>57</sup>Co/Rh Mössbauer source was used. The velocity scale and Mössbauer parameters refer to the metallic  $\alpha$ -Fe absorber at 20 °C. Deconvolution of Mössbauer spectra was performed using the *MossWin* program.

**Table 1.** Experimental conditions for forced hydrolysis of 0.2 M FeCl<sub>3</sub> solutions.

Sample	V(FeCl <sub>3</sub> , 2M) / mL	SDS <sup>(a)</sup> / g	V(H <sub>2</sub> O) / mL	t / °C	Time of ageing / h <sup>(b)</sup>
R1	4		36	160	2
R2	4		36	160	6
R3	4		36	160	24
R4	4		36	160	72
S1	4	0.4	36	160	2
S2	4	0.4	36	160	4
S3	4	0.4	36	160	6
S4	4	0.4	36	160	10
S5	4	0.4	36	160	16
S6	4	0.4	36	160	24
S7	4	0.4	36	160	72

<sup>(a)</sup> SDS = sodium dodecyl sulphate.

<sup>(b)</sup> h = hour.

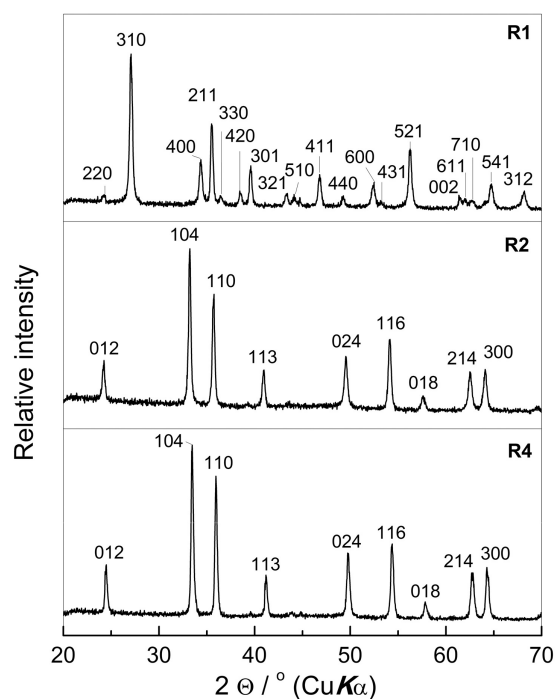


Figure 1. XRD patterns of reference samples R1, R2 and R4.

FT-IR spectra were recorded at RT with a *Perkin-Elmer* spectrometer (model 2000). The powders were mixed with KBr, then pressed into tablets using the Carver press.

The samples were also inspected with a thermal field emission scanning electron microscope (FE SEM, model JSM-7000F) manufactured by *Jeol* Ltd.

## RESULTS AND DISCUSSION

The XRD patterns of reference samples R1, R2 and R4 are given in Figure 1 corresponding to single phases of  $\beta$ -FeOOH (sample R1) or to  $\alpha$ -Fe<sub>2</sub>O<sub>3</sub> (samples R2 and R4).

The Mössbauer spectra of reference samples R1 to R4 produced in the absence of SDS surfactant are shown in Figure 2. The Mössbauer spectrum of sample R1 shows the superposition of two doublets with quadrupole splittings  $\Delta_1 = 0.55$  and  $\Delta_2 = 0.99$  mm s<sup>-1</sup>. The parameters of this spectrum can be assigned to  $\beta$ -FeOOH (Table 2). The spectra of samples R2, R3 and R4 are characterised by one sextet with parameters corresponding to  $\alpha$ -Fe<sub>2</sub>O<sub>3</sub>. The increase in the hyperfine magnetic field (HMF) from 51.2 to 51.5 T (Table 2) with the autoclaving time prolonged from 6 to 72 h can be related to crystalline ordering in  $\alpha$ -Fe<sub>2</sub>O<sub>3</sub>.

Table 2. <sup>57</sup>Fe Mössbauer parameters for reference samples (R) and (S) obtained by precipitation in the presence of SDS.

Sample	Line	$\delta$ / mms <sup>-1</sup>	$\Delta$ or $E_q$ / mm s <sup>-1</sup>	HMF / T	$\Gamma$ / mm s <sup>-1</sup>	A / %	Identification	
R1	Q1	0.38	0.55		0.30	57	$\beta$ -FeOOH	
	Q2	0.37	0.99		0.33	43		
R2	M	0.37	-0.21	51.2	0.34	100	$\alpha$ -Fe <sub>2</sub> O <sub>3</sub>	
R3	M	0.36	-0.21	51.5	0.29	100	$\alpha$ -Fe <sub>2</sub> O <sub>3</sub>	
R4	M	0.37	-0.21	51.5	0.34	100	$\alpha$ -Fe <sub>2</sub> O <sub>3</sub>	
S1	Q <sup>(a)</sup>	0.38	0.79		0.23	100	$\beta$ -FeOOH	
S2	Q <sup>(a)</sup>	0.38	0.81		0.48	85	$\beta$ -FeOOH	
	M1	0.37	-0.26	36.7	1.14	5		$\alpha$ -FeOOH
	M2	0.37	-0.21	48.1	0.58	10		$\alpha$ -Fe <sub>2</sub> O <sub>3</sub>
S3	Q <sup>(a)</sup>	0.38	0.75		0.54	39	$\beta$ -FeOOH	
	M1	0.37	-0.26	37.4	0.97	5		$\alpha$ -FeOOH
	M2	0.37	-0.20	48.5	0.31	56		$\alpha$ -Fe <sub>2</sub> O <sub>3</sub>
S4	Q	0.37	1.18		0.53	4.7		
	M <sup>(a)</sup>	0.37	-0.21	48.3	0.29	95.3		$\alpha$ -Fe <sub>2</sub> O <sub>3</sub>
S5	M <sup>(a)</sup>	0.37	-0.20	49.2	0.27	100	$\alpha$ -Fe <sub>2</sub> O <sub>3</sub>	
S6	M <sup>(a)</sup>	0.37	-0.21	49.8	0.27	100	$\alpha$ -Fe <sub>2</sub> O <sub>3</sub>	
S7	M	0.37	-0.21	50.7	0.25	100	$\alpha$ -Fe <sub>2</sub> O <sub>3</sub>	

All data are given relative to  $\alpha$ -Fe standard.

Key:  $\delta$  = isomer shift;  $\Delta$  or  $E_q$  = quadrupole splitting; HMF = hyperfine magnetic field;  $\Gamma$  = line width; A = area under the peaks.

Errors:  $\delta = \pm 0.01$  mm s<sup>-1</sup>;  $\Delta$  or  $E_q = \pm 0.01$  mm s<sup>-1</sup>; HMF =  $\pm 0.2$  T.

<sup>(a)</sup> Fitted with distribution of quadrupole doublets or hyperfine magnetic fields.

Samples S4 and S5 could contain traces of  $\alpha$ -FeOOH, as denoted with arrows (G) in corresponding figures.

Figure 3 shows the FT-IR spectra of reference samples R1 to R4. The FT-IR spectrum of sample R1 can be assigned to  $\beta$ -FeOOH. Sample R1 shows an IR band centred at  $848\text{ cm}^{-1}$ , two shoulders at  $700$  and  $640\text{ cm}^{-1}$  and two shoulders at  $498$  and  $425\text{ cm}^{-1}$ . According to an earlier works<sup>[15,16]</sup> the band at  $848\text{ cm}^{-1}$  and the shoulder at  $700\text{ cm}^{-1}$  can be assigned to the deformation vibration of OH groups, whereas the intense shoulder at  $640\text{ cm}^{-1}$  can be related to the interaction of Fe-OH groups with  $\text{Cl}^-$  ions.

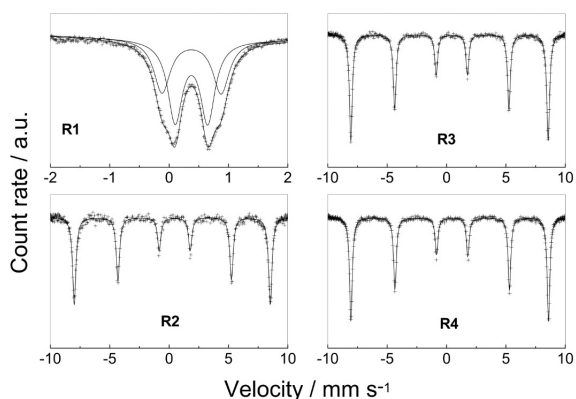


Figure 2.  $^{57}\text{Fe}$  Mössbauer spectra of samples R1 to R4.

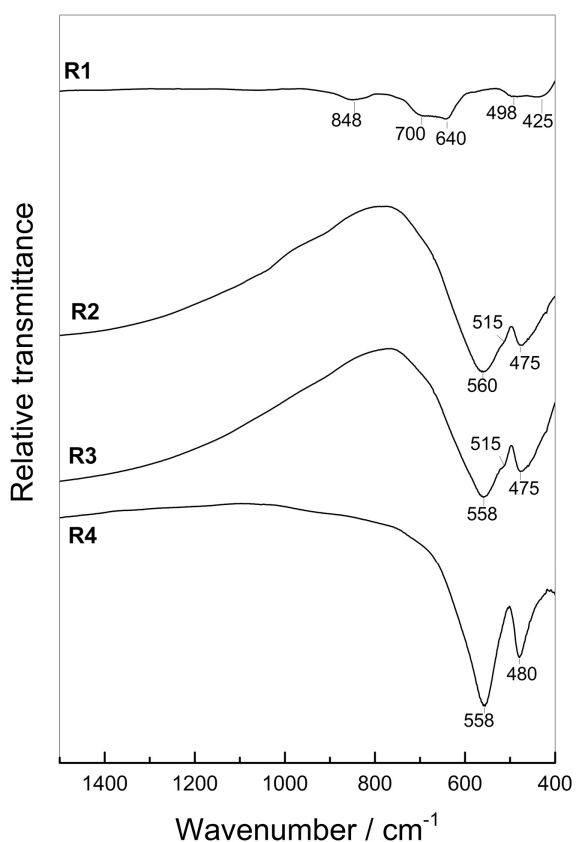


Figure 3. FT-IR spectra of reference samples R1 to R4.

Generally,  $\beta$ -FeOOH exhibits a hollandite-type crystal structure while the structural channels in  $\beta$ -FeOOH produced from the  $\text{FeCl}_3$  solution contain water and a small amount of  $\text{Cl}^-$  ions.<sup>[16]</sup> These  $\text{Cl}^-$  ions (less than  $\sim 2\%$ ) in structural channels stabilize the crystal lattice of  $\beta$ -FeOOH and cannot be removed by simple washing. Weckler and Lutz<sup>[17]</sup> discussed two sets of vibrations at  $847$  and  $820\text{ cm}^{-1}$ , and also those at  $697$  and  $644\text{ cm}^{-1}$  in terms of two  $\text{O-H}\cdots\text{Cl}$  hydrogen bonds present in  $\beta$ -FeOOH. The IR spectrum of  $\beta$ -FeOOH was also the subject of discussion by Murad and Bishop.<sup>[18]</sup> The FT-IR spectra of samples R2 to R4 can be assigned to  $\alpha$ - $\text{Fe}_2\text{O}_3$ . Wang *et al.*<sup>[19]</sup> tabulated optical parameters for bulk  $\alpha$ - $\text{Fe}_2\text{O}_3$  and investigated the influence of the geometrical shape of  $\alpha$ - $\text{Fe}_2\text{O}_3$  particles on the corresponding FT-IR spectrum. Generally, the IR spectrum of  $\alpha$ - $\text{Fe}_2\text{O}_3$  shows six active vibrations, two  $A_{2u}$  ( $E \parallel C$ ) and four  $E_u$  ( $E \perp C$ ).

The XRD patterns of selected samples S1, S2, S4, S6 and S7, prepared in the presence of SDS, are shown in Figure 4. The effect of adding SDS to the precipitation systems is clearly visible. The sharpness of XRD lines of sample S1 is decreased in relation to sample R1, which can be related to lower crystallinity and/or decreased crystallite size of  $\beta$ -FeOOH particles. This can also be related to different integral intensities between XRD lines 310 and 211 for  $\beta$ -FeOOH in sample R1 relative to S1 and S2 (Figures 1 and 4). Additionally, XRD patterns of sample S2 showed the presence of very small amounts of goethite (G) and hematite (H). After 10 h of forced hydrolysis a small amount of  $\alpha$ -FeOOH (sample S4) was also visible in the corresponding XRD pattern (line 110). XRD patterns of samples S6 and S7 showed the presence of  $\alpha$ - $\text{Fe}_2\text{O}_3$  as a single phase.

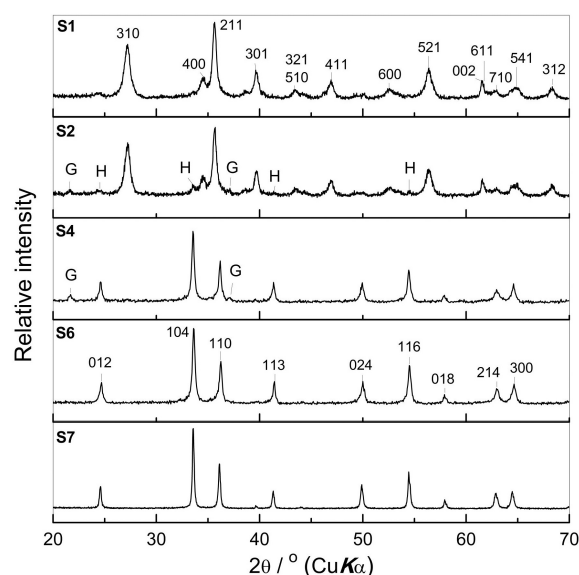
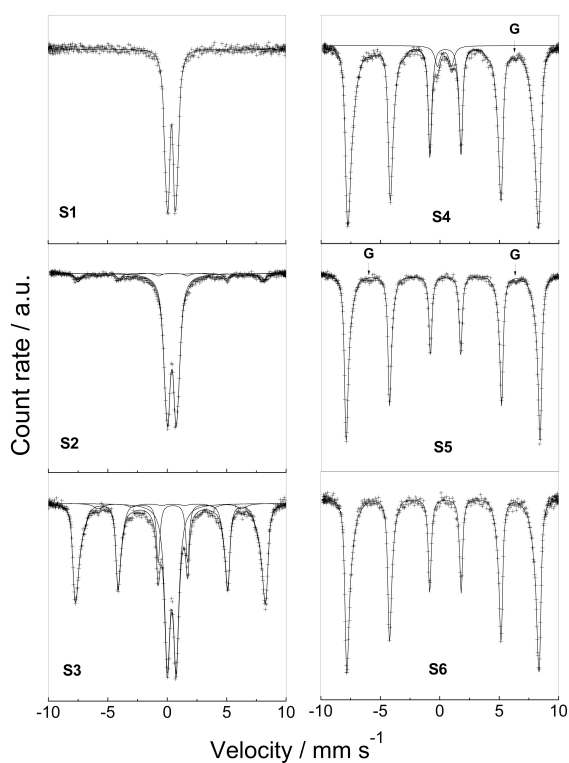


Figure 4. XRD patterns of selected samples S1, S2, S4, S6 and S7 prepared in the presence of SDS. (H = hematite; G = goethite).

Figures 5 and 6 show the Mössbauer spectra of samples S1 to S7. Upon 2h of forced hydrolysis of the 0.2 M FeCl<sub>3</sub> solution containing SDS surfactant (sample S1) a central quadrupole doublet was recorded. This spectrum was fitted for one average doublet with  $\delta = 0.79 \text{ mm s}^{-1}$  (Table 2) and could be assigned to  $\beta\text{-FeOOH}$ .<sup>[20]</sup> The spectrum of sample S2 was fitted as a superposition of the central quadrupole doublet and two sextets. The central quadrupole doublet ( $\Delta = 0.81 \text{ mm s}^{-1}$ ) could be assigned to  $\beta\text{-FeOOH}$  (85 %), whereas the two sextets of very small intensities with HMF = 36.7 T (5 %) and HMF = 48.1 (10 %) can be assigned to  $\alpha\text{-FeOOH}$  and  $\alpha\text{-Fe}_2\text{O}_3$ , respectively. Upon further prolongation of autoclaving time up to 6 h there was a decrease in  $\beta\text{-FeOOH}$  to 39 % and a corresponding increase in  $\alpha\text{-Fe}_2\text{O}_3$  to 56 %, whereas  $\alpha\text{-FeOOH}$  remained at 5 % (sample S3). In sample S4 the  $\alpha\text{-Fe}_2\text{O}_3$  fraction increased to 95.3 %. The same spectrum also showed central quadrupole doublet with  $\Delta = 1.18 \text{ mm s}^{-1}$  (4.7 %). In line with XRD pattern the peak denoted as G in the Mössbauer spectrum of sample S4 could be assigned to  $\alpha\text{-FeOOH}$ . Mössbauer spectrum of sample S7 corresponds to  $\alpha\text{-Fe}_2\text{O}_3$  as a single phase (Figure 6). The HMF values of the  $\alpha\text{-Fe}_2\text{O}_3$  phase increased from 48.1 T (samples S2) to 50.7 (sample S7), thus indicating a much lower degree of  $\alpha\text{-Fe}_2\text{O}_3$  crystallinity in relation to reference samples R2 to R4 (51.2 to 51.5 T).



**Figure 5.** <sup>57</sup>Fe Mössbauer spectra of samples S1 to S6 prepared in the presence of SDS.

The effect of SDS is also visible in the FTIR spectra shown in Figure 7. The spectrum of sample S1 can be

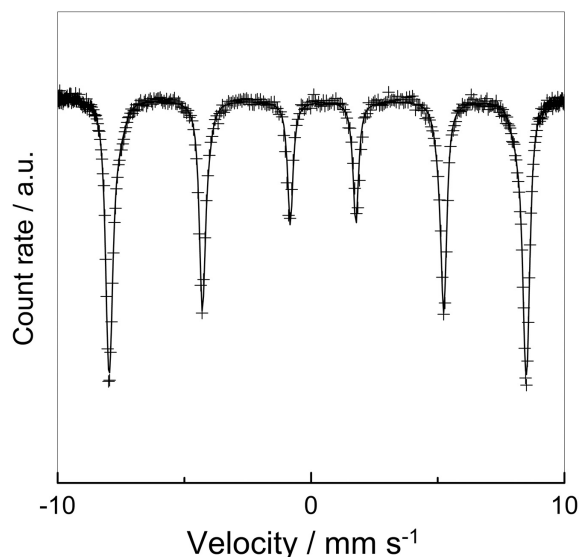


**Figure 6.** <sup>57</sup>Fe Mössbauer spectrum of sample S7 prepared in the presence of SDS.

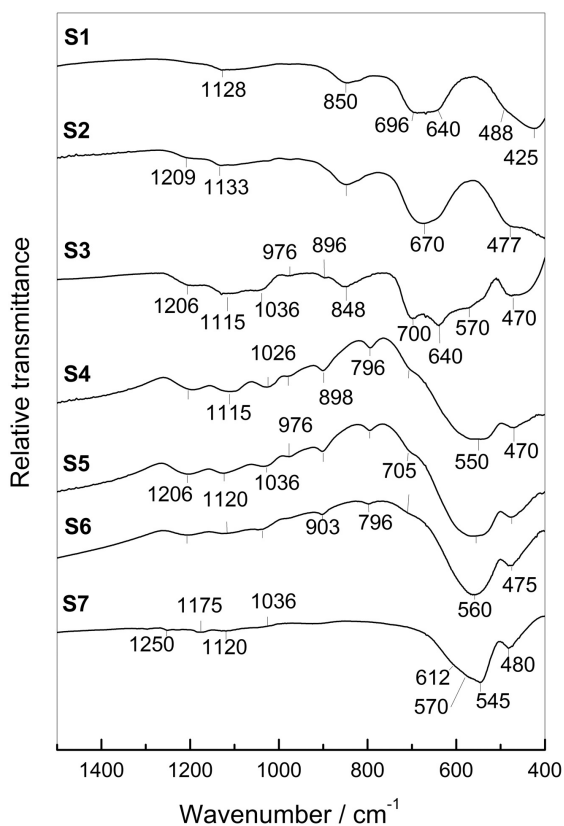


**Figure 7.** FT-IR spectra of samples S1 to S7 prepared in the presence of SDS.

assigned to the  $\beta$ -FeOOH phase. The only difference between samples S1 and S2 is in the relative intensities of the shoulders at 696, 640 and 488, 425  $\text{cm}^{-1}$ . Additionally, the IR bands at 1128  $\text{cm}^{-1}$  (sample S1) and 1209, 1133  $\text{cm}^{-1}$  (sample S2) are also visible. Sample S3 shows IR bands that can be assigned to  $\beta$ -FeOOH and two additional IR bands at 570 and 470  $\text{cm}^{-1}$  that can be assigned to  $\alpha$ -Fe<sub>2</sub>O<sub>3</sub>.<sup>[21]</sup> The IR band at 896  $\text{cm}^{-1}$  could be assigned to a small amount of the  $\alpha$ -FeOOH phase, but the second IR band close to 800  $\text{cm}^{-1}$ , also typical of  $\alpha$ -FeOOH, is not visible due to the overlapping with a broad IR band of  $\beta$ -FeOOH centred at 848  $\text{cm}^{-1}$ .<sup>[17]</sup> Generally, the IR band of  $\alpha$ -FeOOH centred at 896  $\text{cm}^{-1}$  is assigned to the *in-plane* Fe–O–H bending band ( $\delta_{\text{OH}}$ ), whereas the *out-of-plane* bending band ( $\nu_{\text{OH}}$ ) is typically around 800  $\text{cm}^{-1}$ .<sup>[21]</sup> In the FT-IR spectra of samples produced in the presence of SDS additional bands are also noticed. For example, in the spectrum of sample S3 four IR bands at 1206, 1115, 1036 and 976  $\text{cm}^{-1}$  are well visible. These IR bands can be related to the sulphate group. The  $\nu_3(\text{SO}_4)$  fundamental vibration is split into 3 active IR bands due to the formation of a surface bidentate bridging complex between the sulphate group and surface iron atoms.<sup>[22]</sup> The presence of an IR band at 977  $\text{cm}^{-1}$  is due to the  $\nu_1(\text{SO}_4)$  vibration. It is generally known that the specific adsorption of oxyanions reaches its maximum at acidic pH values and decreases with an increase in pH values.

Generally, it is also known that the presence of oxyanions, surface active or complexing agents may strongly influence the shape of hematite particles in precipitation processes. For example, Ocaña *et al.*<sup>[23]</sup> precipitated spindle-shaped  $\alpha$ -Fe<sub>2</sub>O<sub>3</sub> particles by a forced hydrolysis of the Fe(ClO<sub>4</sub>)<sub>3</sub> solution at 100 °C. The phosphate anions that could not be washed out were discussed as responsible for the formation of spindle-shaped particles. The adsorbed phosphates were visible in the IR spectrum as evidence, with several peaks between 1036 and 934  $\text{cm}^{-1}$ . In the present work Mössbauer, XRD and FT-IR measurements showed a direct phase transformation  $\beta$ -FeOOH  $\rightarrow$   $\alpha$ -Fe<sub>2</sub>O<sub>3</sub> in reference samples (R) produced by the forced hydrolysis of the 0.2 M FeCl<sub>3</sub> solution. In the presence of SDS (samples S1 to S7) the kinetics of this phase transformation was retarded and in samples produced between 4 and 24 hours of forced hydrolysis a small fraction (traces) of an intermediate phase  $\alpha$ -FeOOH were detected. The HMF values of  $\alpha$ -Fe<sub>2</sub>O<sub>3</sub> particles prepared in the presence of SDS varied from 48.1 to 50.7 T. These HMF values were significantly below 51.75 T measured for well-crystalline  $\alpha$ -Fe<sub>2</sub>O<sub>3</sub>, as reported by Murad and Johnston.<sup>[24]</sup> It can be concluded that the presence of SDS lowers the crystallinity of precipitated  $\alpha$ -Fe<sub>2</sub>O<sub>3</sub>. Musić *et al.*<sup>[25]</sup> investigated the effect of HCl additions on the forced hydrolysis of FeCl<sub>3</sub> solutions. They found out that under certain conditions the forced hydrolysis of the FeCl<sub>3</sub> solution containing only HCl additions can

also produce an  $\alpha$ -FeOOH phase. Wang *et al.*<sup>[26]</sup> investigated the precipitation of  $\alpha$ -Fe<sub>2</sub>O<sub>3</sub> nanoparticles by the forced hydrolysis of FeCl<sub>3</sub> solutions with no additive presence. In dependence on experimental conditions, primary nanoparticles showed different morphologies. Beside the  $\beta$ -FeOOH  $\rightarrow$   $\alpha$ -Fe<sub>2</sub>O<sub>3</sub> phase transformation there was also a direct phase transformation of the amorphous fraction

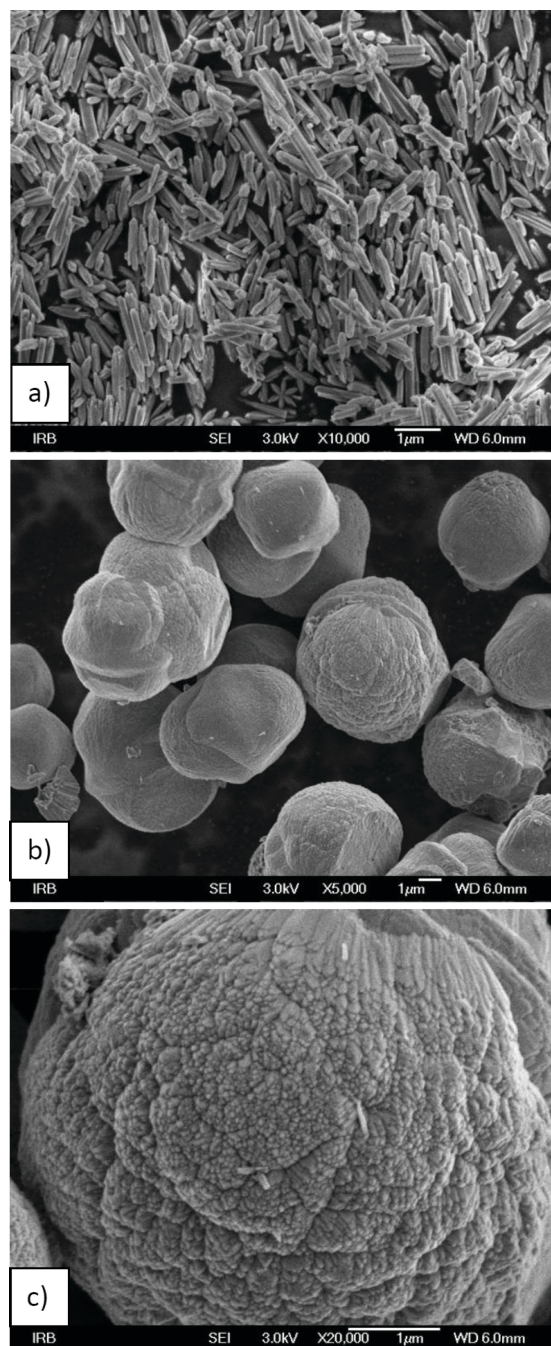


**Figure 8.** FE SEM images of (a) sample R1 and (b, c) sample R2.

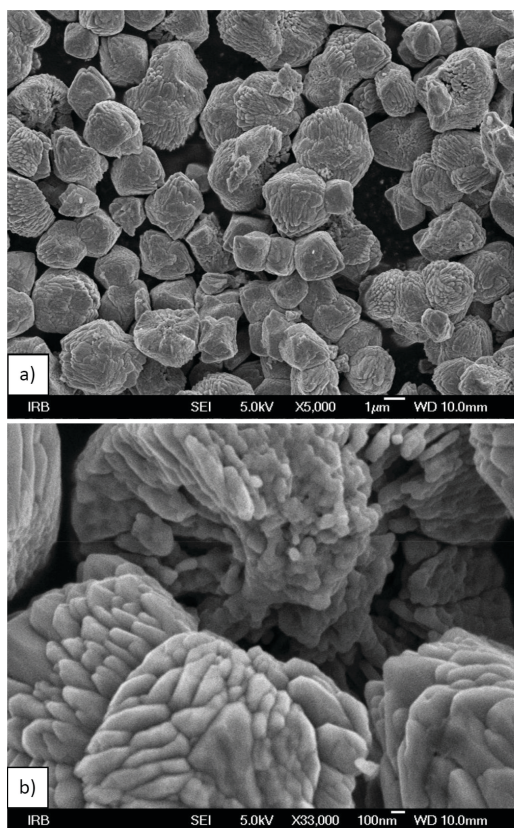


Figure 9. FE SEM images of (a,b) sample R4.

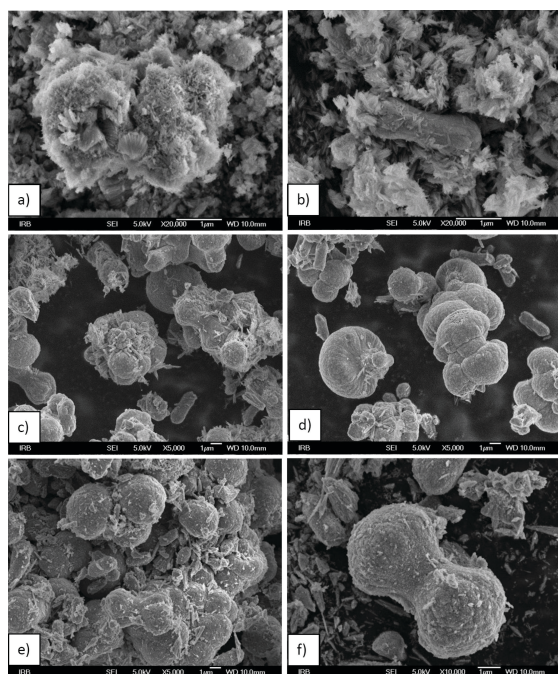


Figure 10. FE SEM images of (a) sample S1, (b) sample S2, (c) sample S4, (d) sample S5 and (e,f) sample S7 precipitated in the presence of SDS.

into  $\alpha$ -Fe<sub>2</sub>O<sub>3</sub>. In the present work the addition of SDS to the precipitation system caused the formation of a small fraction of  $\alpha$ -FeOOH as an intermediate phase, which at a prolonged time of autoclaving was transformed into  $\alpha$ -Fe<sub>2</sub>O<sub>3</sub> by way of the dissolution/recrystallization mechanism.

The FE SEM image of sample R1 (Figure 8a) showed the dominant presence of  $\beta$ -FeOOH rods, but star- and X-shaped particles were also noticed. Sample R2 showed micron size  $\alpha$ -Fe<sub>2</sub>O<sub>3</sub> particles (Figure 8b) which consisted of primary  $\alpha$ -Fe<sub>2</sub>O<sub>3</sub> nanoparticles (elongated), as evidenced by Figure 8c.  $\alpha$ -Fe<sub>2</sub>O<sub>3</sub> particles produced upon 72 h of the forced hydrolysis of FeCl<sub>3</sub> solutions at 160 °C (sample R4) are shown in Figure 9a. These particles also showed a substructure (Figure 9b); however, the primary  $\alpha$ -Fe<sub>2</sub>O<sub>3</sub> particles increased in size. Figure 10 shows the FE SEM images of selected samples prepared in the presence of SDS. The FE SEM image of sample S1 (Figure 10a) shows the aggregates of very fine  $\beta$ -FeOOH needles. In addition to very fine  $\beta$ -FeOOH needles, Figure 10b (sample 10b), also shows peanut particles of  $\alpha$ -Fe<sub>2</sub>O<sub>3</sub>. The substructure of these peanut particles consisting of laterally arrayed subparticles is visible. The FE SEM images of samples S4 and S5, respectively, are shown in Figures 10c,d, demonstrating the predominant presence of big  $\alpha$ -Fe<sub>2</sub>O<sub>3</sub> particles of different morphologies (spheres, double cupolas with ring and peanut shaped particles). Similar shapes of  $\alpha$ -Fe<sub>2</sub>O<sub>3</sub> particles are also visible in the FE SEM images of sample S7 (Figure 10e,f).

## CONCLUSION

The effect of SDS (1 %) on the kinetics, phase composition and shape of the particles precipitated by the forced hydrolysis of the 0.2 M FeCl<sub>3</sub> solution was investigated. A direct phase transformation  $\beta$ -FeOOH  $\rightarrow$   $\alpha$ -Fe<sub>2</sub>O<sub>3</sub> *via* dissolution/recrystallization was present in the absence of SDS. On the other hand, in the presence of SDS this transformation was retarded in relation to reference kinetics. In the presence of SDS a small fraction of  $\alpha$ -FeOOH precipitated, which was transformed into the end product  $\alpha$ -Fe<sub>2</sub>O<sub>3</sub> also *via* the dissolution / recrystallization mechanism.  $\alpha$ -Fe<sub>2</sub>O<sub>3</sub> particles precipitated in the presence of SDS showed lower crystallinity in relation to reference samples, as concluded on the basis of the Mössbauer spectra. This effect was explained by a competition between the stability of Fe(III)-dodecyl sulphate on one side and the formation of iron oxide phases on the other. Precipitated  $\alpha$ -Fe<sub>2</sub>O<sub>3</sub> particles showed a substructure, *i.e.*, consisted of much smaller primary particles. The effect of SDS on the microstructure of  $\alpha$ -Fe<sub>2</sub>O<sub>3</sub> particles was noticed. The influence of SDS on the forced hydrolysis of FeCl<sub>3</sub> solutions can be related to the specific adsorption of sulphate groups on the nuclei and crystallites of FeOOH and  $\alpha$ -Fe<sub>2</sub>O<sub>3</sub> phases. The steric effect of *n*-alkyl chain cannot be excluded. This work also showed

how the important is combination of XRD, Mössbauer and FT-IR spectroscopic methods in the analysis of small amounts (traces) of iron oxides produced in the precipitation processes.

**Acknowledgment.** This work was supported by the Croatian Science Foundation: Project No. IP-2016-06-8254 and European Regional Development Fund – the Competitiveness and Cohesion Operational Programme: Project No. KK.01.1.1.01.0001.

## REFERENCES

- [1] J. R. Freyer, A. Gildawie, R. Paterson, *High resolution studies of the initial stages of precipitation of hydrous iron oxides*, Eighth Int. Congress on Electron Microscopy, Canberra, **1974**, *1*, 708.
- [2] J. M. González-Calbet, M. A. Alario-Franco, M. Gayoso-Andrade, *J. Inorg. Nucl. Chem.* **1981**, *43*, 257.
- [3] S. Musić, A. Vértes, G. W. Simmons, I. Czako-Nagy, H. Leidheiser Jr., *J. Coll. Interface Sci.* **1982**, *85*, 256.
- [4] E. Matijević, P. Scheiner, *J. Coll. Interface Sci.* **1978**, *63*, 509.
- [5] S. Hamada, E. Matijević, *J. Chem. Soc. Faraday Trans. I* **1982**, *78*, 2147.
- [6] E. K. De Blanco, M. A. Blesa, S. J. Liberman, *Reactivity of Solids* **1986**, *1*, 189.
- [7] S. Musić, M. Ristić, S. Krehula, *Mössbauer Spectroscopy: Applications in Chemistry, Biology and Nanotechnology* (Eds. V. K. Sharma, G. Klingelhofer, T. Nishida), John Wiley & Sons, **2013**, 34.
- [8] H. Katsuki, S. Komarneni, *J. Am. Ceram. Soc.* **2003**, *86*, 183.
- [9] T. Sugimoto, Y. Wang, H. Itoh, A. Muramatsu, *Colloids Surfaces A: Physicochem. and Eng. Aspects*, **1998**, *134*, 205.
- [10] B. Mao, Z. Kang, E. Wang, C. Tian, Z. Zhang, C. Wang, Y. Song, M. Li, *J. Solid State Chem.* **2007**, *180*, 489.
- [11] K. Kandori, N. Hori, T. Ishikawa, *Colloids Surfaces: Physicochem. Eng. Aspects* **2006**, *290*, 280.
- [12] K. Kandori, I. Hori, A. Yasukawa, T. Ishikawa, *J. Mater. Sci.* **1995**, *30*, 2145.
- [13] M. Žic, M. Ristić, S. Musić, *J. Alloys Comp.* **2008**, *464*, 81.
- [14] M. Žic, M. Ristić, S. Musić, *J. Mol. Struct.* **2008**, *924-926*, 235.
- [15] S. Musić, A. Šarić, S. Popović, *J. Mol. Struct.* **1997**, *410-411*, 153.
- [16] A. Šarić, S. Musić, K. Nomura, S. Popović, *Mater. Sci. Eng. B.* **1998**, *56*, 43.
- [17] B. Weckler, H.D. Lutz, *Eur. J. Solid State Inorg. Chem.* **1998**, *35*, 531.
- [18] E. Murad, J.L. Bishop, *Am. Mineral.* **2000**, *85*, 716.
- [19] Y. Wang, A. Muramatsu, T. Sugimoto, *Colloid Surf. Sci. A: Physicochem. Aspects* **1998**, *134*, 281.
- [20] E. Murad, *Clay Minerals* **1979**, *14*, 273.
- [21] S. Krehula, S. Musić, *J. Cryst. Growth* **2008**, *310*, 513.
- [22] D. Peak, R. G. Ford, D. L. Sparks, *J. Coll. Interface Sci.* **1999**, *218*, 289.
- [23] M. Ocaña, M. P. Morales, C. J. Serna, *J. Coll. Interface Sci.* **1999**, *212*, 317.
- [24] E. Murad, J. H. Johnston, *Mössbauer Spectroscopy Applied to Inorganic Chemistry Vol 2* (Ed. G. J. Long), Plenum Pub. Corp. **1987**, 75.
- [25] S. Musić, S. Krehula, S. Popović, *Mater. Lett.* **2004**, *58*, 2640.
- [26] W. Wang, J.Y. Howe, B. Gu, *J. Phys. Chem. C* **2008**, *112*, 9203.